LIP-STUDENTS-23-00

The first miniTrasgo Cosmic Ray detector

Víctor M. Nouvilas and Cayetano Soneira[1,a]

[1] *Complutense University of Madrid, Spain*

Project supervisor: Alberto Blanco

October 13, 2023

Abstract. The study of cosmic rays, originating from various sources including the Sun and beyond, remains a field with unanswered questions. To probe these high-energy particles, Extensive Air Showers (EAS) generated by cosmic ray interactions with Earth's atmosphere are analyzed. As part of the TRASGO (TRAck reconStructinG bOx) project, this paper introduces the miniTRASGO cosmic ray telescope, a portable version of the concept employing Resistive Plate Chambers (RPCs) for particle detection. The telescope measures both muons and electrons, offering potential insights into cosmic ray behavior. Challenges and possibilities of Ultra-High Energy Cosmic Rays (UHECRs) detection are discussed. The telescope's design, RPC structure, and measurement techniques are detailed, including intrinsic efficiency, charge spectra analysis and a first insight into multiple particle events. Future work includes implementing a full database and query system, refining interstrip measurements, continue exploring higher-order multiplicities and calculating a robust cosmic ray rate.

Keywords: Gaseous detectors, Cosmic Rays, Resistive plate chamber, Ground telescope

1 Introduction

The study of cosmic rays, which comprise particles arriving from the Sun, our Galaxy, and beyond, remains a field with lingering unknowns. These particles, including protons, atomic nuclei, electrons, and positrons, possess energies surpassing 10^{20} eV, far beyond current acceleration technologies. One possibility for investigating these enigmatic particles relies on analyzing Extensive Air Showers (EAS) generated when cosmic rays interact with Earth's atmosphere. These showers are composed of secondary particles and demand extensive detection arrays due to their wide spread. While methods for measuring primary cosmic rays exist, they often involve expensive setups. J. Linsley proposed a viable alternative – mini detector arrays coupled with parameterized correlations [5]. Recent advancements even suggest the potential of smaller, high-resolution tracking detectors for improving EAS analysis [6]. This paper a new, small RPC-based telescope to study these phenomena.

1.1 The TRASGO project

The TRASGO (TRAck reconStructinG bOx) project is focused on advancing cosmic ray (CR) detectors using cutting-edge technologies from High Energy Particle Physics. It is embedded in CASTRO, Cosmic rAy Survey TRasgo netwOrk, a new, international collaboration made up of members from Spain, Poland and Mexico, among others.

The TRASGO concept incorporates Resistive Plate Chambers (RPCs), a cost-effective type of gas ionization detector known for its performance. The basic RPC is made of two layers of resistive material, such as glass, separated by a gas gap where a high voltage is applied. The main goal of TRASGO is to create versatile tools for acquisition, monitoring, event reconstruction, and data analysis regardless of detector design. In contrast to conventional CR detectors, **TRASGOs measure both muons and electrons**. While they could detect high-energy gamma particles, simulations show these contributions are minor. The objective is that the software aids in identifying muons and electrons, and adding lead layers may improve particle identification.

Further details about TRASGO detectors can be found in the original planning article, [7], and in a more recent status review, [8].

1.2 Charged Secondary Cosmic Rays

Muon particles, which arise as byproducts of primary cosmic ray collisions in Earth's atmosphere, exhibit remarkable penetrative qualities, reaching subterranean depths of several kilometers. Originating from the decay of mesons, especially pions and kaons, created in subsequent nuclear interactions after initial atmospheric contact at approximately 15-20 km altitude, muons are unstable. Some lower-energy muons may decay into electrons prior to reaching the Earth's surface. The production rate of muons is governed by atmospheric density, while their decay probability correlates with the altitude of their formation.

Measuring the primary cosmic ray rate through muon observations mandates adjustments for atmospheric pressure and temperature. The successful arrival of muons at ground level requires high-energy primary protons, with energy requisites varying based on observation latitude. Although muon detectors are less prevalent in monitoring solar activity compared to neutron detectors, their advantage lies in the traceable paths of their arrival. Leveraging just a few directional telescopes enables comprehensive sky coverage, facilitating the visualization of magnetized solar plasma clouds and the potential anticipation of magnetic storms hours ahead.

[a] e-mail: csoneira@ucm.es

Figure 1. miniTRASGO picture.

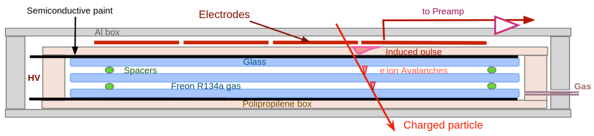

Figure 2. RPC layout (not to scale).

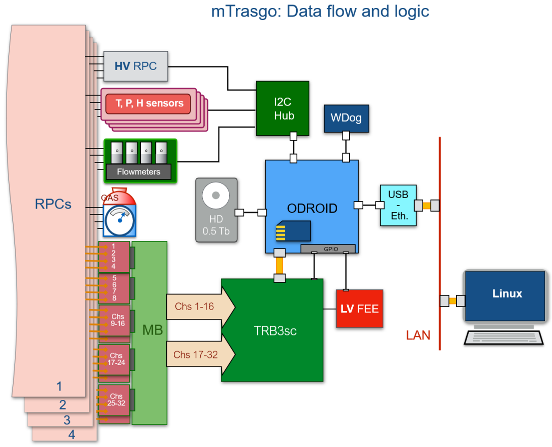

Figure 3. Scheme of the miniTRASGO system.

Electrons, often overlooked within secondary cosmic radiation, possess intrinsic value as a primary cosmic ray information source. Despite their limited mean free path causing origin information loss due to directional shifts and gamma emission via Bremsstrahlung, high-energy electrons are derived from muon decay. This offers an indirect means of gauging decaying muons. Thorough assessment of electrons, encompassing energy distribution, arrival direction, and background electron groupings, presents an avenue to tap into novel and valuable cosmic ray and atmospheric data.

2 The miniTRASGO system

The miniature TRASGO, miniTRASGO from now on, depicted in Fig. 1, consists of four multigap RPC modules [2], each of them confined in a permanently sealed plastic gas tight box equipped with feed-throughs for gas and High Voltage (HV) connections. Each RPC module has two gas gaps defined by three 2 mm thick float glass electrodes of about 300 × 300 mm^2 separated by 1 mm nylon mono-filaments. The HV electrodes are made up of a semi-conductive layer (Based on an artistic acrylic paint with around 10 MΩ/cm^2 applied to the outer surface of the outermost glass panes with airbrush techniques.

Each of the four modules are read out by a signal pickup electrode equipped, in one side, with 4 asymmetric copper strips (one 98 mm wide, the rest 63 mm wide; 300 mm long) located on top of each one of the modules. The complete structure is enclosed in an aluminium box that provides the necessary electromagnetic insulation and mechanical rigidity. In Fig. 2 a schematic of the inner structure of the module is shown.

The strips on both sides are read using high-speed Front End Electronics (FEE) as outlined in [3]. These electronics encode two crucial parameters into a single output signal: time (leading edge) with precision better than 30 ps and charge (pulse width). To determine the charge, Time over Threshold (ToT) is measured on an amplified signal copy, integrated with an integration constant of approximately 100 ns. The resultant signals, in LVDS (Low Voltage Differential Signal) standard, are then processed by a TDC-and-Readout Board (TRB) version 3sc, equipped with 32 multihit Time-to-Digital Converter (TDC) channels utilizing TDC-in-FPGA technology, ensuring a time precision of under 20 ps (?). This TRB3sc, functioning as a logic unit and trigger distributor, forms an independent Data Acquisition (DAQ) system.

The RPCs were operated within an open gas loop using R134a (1,1,1,2-Tetrafluoroethane, $C_2H_2F_4$). The operational point of the detector was determined to be approximately 2800 kV/gap. The system counts with environmental sensors such a termometer, a relative humidity meter and a barometer. It also has flowmeters to check the gas flow as it goes out of the open R134a circuit. A complete scheme of the system is shown in Fig. 3.

3 Measuring with miniTRASGO

In this section the main magnitudes measurable by the telescope are discused, as well as the calibration process involved in the treatment of the data.

3.1 The product of the measurement

It is said that a RPC (any of the four) has a **detection** when any of the four strips that constitute the RPC, on any of both Front (F) or Back (B) sides, receives a signal. This signal comes from a **hit** along the strip. The **trigger** is defined as the criteria chosen to register an **event**. In this

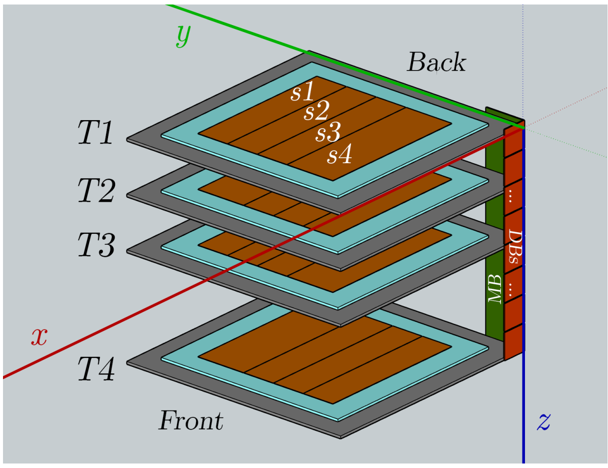

Figure 4. Name and axis convention. Note that the distance between planes 3 and 4 is the double of the other distances between planes.

current setup, the trigger is determined by getting a detection, in a time window of at least 30 ns, in three of the four RPCs.

For each RPC strip i, with signal in F or B sides, there are both leading and tailing of the signal, from which time and charge can be obtained, respectively. Both magnitudes are obtained in ns, so charge is actually in arbitrary units (AU). The time measure for each side of the strip is relative to the trigger time, so it gives no physical information by itself if it is not accompanied by time measure of the other side of the strip.

From time, when it is measured on both sides, the position of the interaction along the strip can be determined. Charge is not proportional to energy: it has a distribution dependent on the number of strips triggered, so it can be used in terms of monitoring and, more importantly, to choose the strip where the particle interacted in case several strips receive signal in the same RPC.

In this context, there are, given a raw event, five possible types of detections on a RPC: no strip receives signal, only one does (*single*), two (*double*), three (*triple*)... up to four strips in the same RPC receiving a signal (*quadruple*). Double, triple and quadrupole are framed inside the *multistrip* detections. This distinction is key since some multistrip detections can possibly be associated with more than one particle: it is said then that the detection has multiplicity n being this the number of particles involved. It is possible, though, that there is crosstalk: a capacitive coupling between strips that is seen in data as a very small leaking of charge from one strip to another. In this case it is interesting to consider this double strip detection as actually a single strip detection. Classification is crucial for another reason: the relatively wide strips allow us to capture a few instances of double strip detections that cannot be attributed to crosstalk caused by a single particle. In such cases, we assign the hit point to the midpoint between two strips rather than the center, a scenario referred to as *interstrip* detection.

Given a certain RPC, T1, T2, T3 or T4, convention represented in Fig. 4; to choose the strip of the detection, s, in case there is no interstrip, the strip with maximum value of charge is taken, and that charge is calculated as follows:

$$Q = \frac{Q_{F,s} + Q_{B,s}}{2} + \varepsilon^{Q}_{T,s}.$$

$\varepsilon^{Q}_{T,s}$ is the calibration parameter for the charge in strip s and RPC T. Once the strip is assigned, the Y position is determined according to that strip number and the RPC involved: since there is a wider strip that is located in opposite sides from one RPC to another, this selection has to be done carefully. The middle position of each strip is assigned. In case of an interstrip, the position is set at the edge of the strips.

For the longitudinal position along the strip, X, the measured times on the right and left sides of the selected strip are used, $T_{F,s}$ and $T_{B,s}$. To calculate that position, the following equation is used:

$$X = \frac{T_{F,s} - T_{B,s}}{2} \cdot V_{\text{strip}} + \varepsilon^{T}_{T,s},$$

where $\varepsilon^{T}_{T,I}$ is a calibration parameter for that strip s in the RPC T. In practice, though, the parameter is calculated before multiplying by the velocity:

$$\hat{\varepsilon}^{T}_{T,I} = \frac{\varepsilon^{T}_{T,I}}{V_{strip}}$$

Time along the strip and charge, given in ns and AU, respectively, are the main products of a measurement made by the detector. From now on, even it is indicated in ns, the time along the strip will be referred as position along the strip[1]. In this section it has been shown how to operate with them to obtain the most fundamental magnitudes the telescope can provide, those that can be the building blocks for more complicated analysis: the charge of the detection and its position in each RPC.

3.2 Calibration

The calibration procedures are described in this part. The main issue in both position and charge calibrations is to calculate the offset properly. The technique of intrinsic efficiency, though, requires some subtle considerations.

3.2.1 *Position along the strip*

Since time differences between Front and Back of the strip reveal the position of the hit, the calibration procedure is just as follows: time values outside certain quantiles are filtered and then the mean between the extreme values is taken. This is the desired offset. Now, to get the times between 0 and some positive value, a simple translation is done to all values.

[1]To avoid confusion, since exact timestamp of the event is also available.

3.2.2 Charge

In this case all the values below a certain quantile are taken, then promediated: that is the offset considered.

3.2.3 Intrinsic efficiency

This telescope, compared to other detectors of its kind, has the advantage of being composed by four detection planes. This feature makes it possible to calculate the intrinsic efficiency with no external aids, such as scintillators and photomultipliers [1]. Since the trigger is configured to be a detection in at least three of the four RPCs, a efficiency calculation can be designed as follows. To study a certain RPC, the following steps are taken:

1. Check if the other three RPCs received a signal.
2. Check if the position of the hits in the other RPCs are aligned (with a tolerance).
3. Check if that line joining the positions on other RPCs passes through the RPC of interest. If it does, then it sums as *passing*.
4. Check if there is a detection in the RPC of interest and, if there is, if it is aligned with the trajectory described by the other three positions. If it is, it sums as *detected*.

Finally just a quotient between *detected* and *passing* needs to be performed to obtain the intrinsic efficiency value for the RPC that it is being studied.

4 Results

Some interesting figures from the measurements and calibration previously explained allow creating the following figures and results.

4.1 Efficiency

The efficiency is $0.83, 0.96, 0.96$ and 0.83 (CORRECT THIS) for the four RPCs, from T1 to T4, with the current criteria, as explained in the previous section. Fig. 5 shows an event in which the three considered points to calculate the efficiency are aligned and the trajectory passes through the plane of study.

4.2 Position maps

The count rate vs. position maps for the four RPCs are depicted in Fig. 6. This was made by calibrating the position along the strip just as it was explained in the previous section. For now on, only the rate as counts per time interval, corrected by intrinsic efficiency, is considered, though the flux values can be calculated accounting also for the surface of each strip and a rough estimation of the solid angle subtended by each RPC given the trigger condition (it has to be done pointwise).

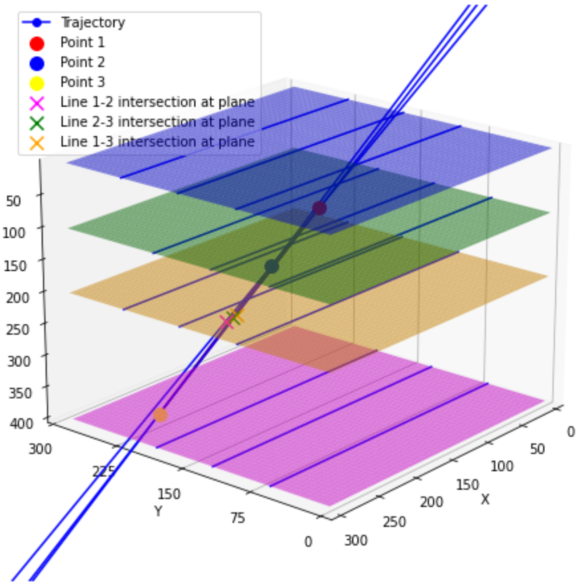

Figure 5. A case classified as *crossing* particle for T3. Seeing if there is a detection in T3 will determine if it sums to the efficiency as *detected* particle.

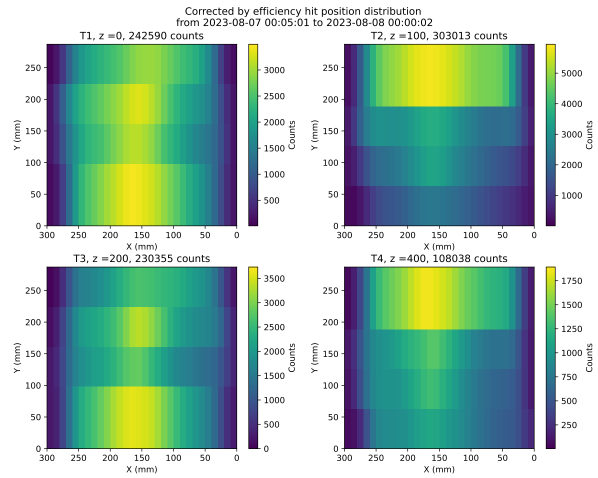

Figure 6. Position maps for the RPCs. The units are counts, and they are corrected by the intrinsic efficiency. A gaussian blurrying is applied in the x direction to visually acount for the uncertainty in the position calculated from the times along the strip.

The different number of events from one RPC to another can be explained mainly by geometrical reasons: the 200 mm that separate T4 from T3 make this bottom RPC the one with the smallest solid angle subtended: ≈ 1.6 sr compared to the ≈ 3.2 sr of T1, T2 and T3; in a rough approximation for the middle of the RPC. This is a factor of 2 that explains the main difference in the count number. A more subtle study is needed to understand the discrepancy between T2 and T3. Geometric reasons, such as the different distance between planes (a constant 100 mm for the T1, T2, T3 planes and 200 mm for the T3 to T4) could be wielded to explain it. Nevertheless, it can not be dis-

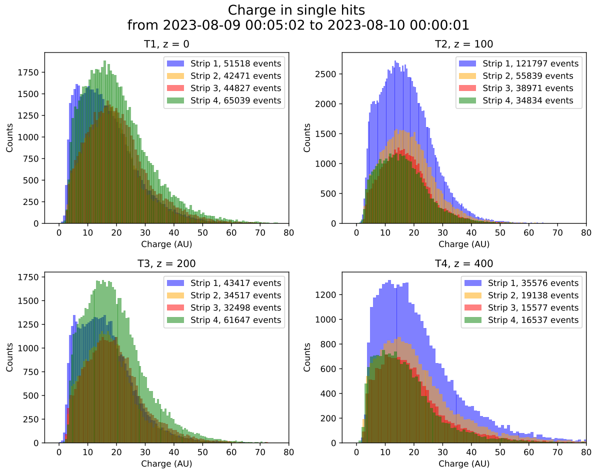

Figure 7. Charge spectra for each RPC and each strip for single hits (those detections triggering only one strip per RPC).

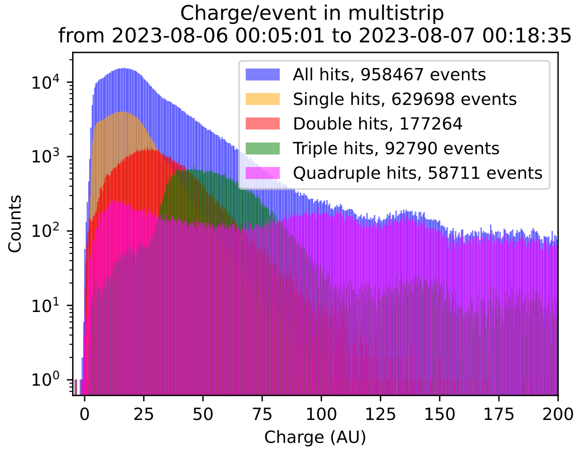

Figure 8. Total-charge spectrum collected per detection (in the whole RPC) according to the number of strips triggered. In logarithmic scale.

carded that it might be a failure in the assembly of T2 that is leading to different electrical magnitudes in the RPC. This question will be furtherly developed below.

4.3 Charge spectra

Just as a representation per RPC and per strip has been performed for the time values (once transformed to position), a new figure with charge spectra per RPC and per strip can be performed. We start, though, with the case of single hit events: those in which the charge is totally collected in only one strip.

4.3.1 Single hits

The Fig. 7 shows the stripwise measure of charges for single hits. The total number of events used to calculate the histogram is indicated in the legend. As it can be seen in the figure, T2, especially the Strip 1, has a lot more counts than the other RPCs. In other words, T2 detects much more single hits than the other RPCs.

4.3.2 Multistrip hits

Just by plotting the charge spectra for each multistrip detection, Fig. 8 can give an idea on the number of events and the charge of each type of hit.

It can be seen that, as the number of strips triggered rises, the most probable charge of the detection in that RPC also goes up while the number of events diminishes, being by a significant difference the single hits the most probable. It is also interesting to note the different shapes of the charge spectra: the double hit distribution is similar to summing two single hit distributions. The triple hits, though, include in the left a tail that suggests actually a double hit detection, while in the right a double bump is shown, indicating potentially different types of **streamers**. The quadruple hits include a left bump suggesting a single event with a significant crosstalk (so all the strips in

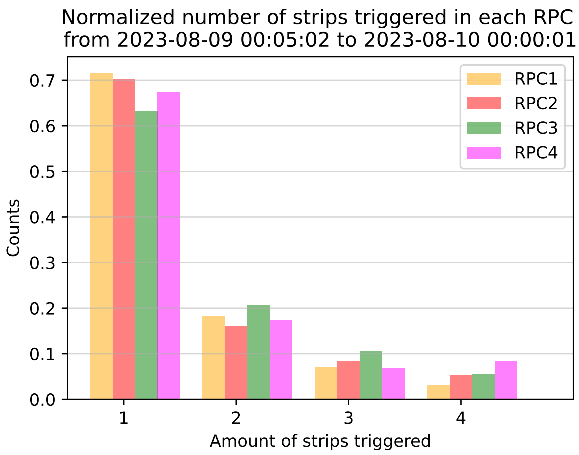

Figure 9. Number of strips triggered according to the RPC. Note the high number of single hits in RPC 2 compared to RPC 1 and RPC 3, closer in position.

a RPC are triggered) and several bumps in the right: the first being that corresponding to a quadruple event typically (since it follows the curve traced by the maxima of single, double and triple hits) and two bumps in the far right that correspond to those of the triple hits.

A representation of the number of strips triggered according to the RPC could also be valuable. This is showed in Fig. 9.

4.3.3 Crosstalk and interstrip characterization

Following the discussion started in the previous part about double hits, a look on Fig. 10 gives a clue on the nature of this events: the shape of the charge distribution is a monotonically decreasing one, and not a typical shape of a charge spectrum.

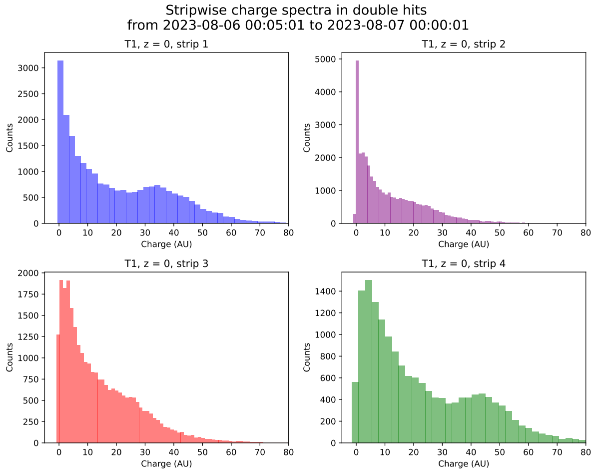

Figure 10. Charge spectrum per strip and per RPC for double hits (those collecting charge in exactly two strips).

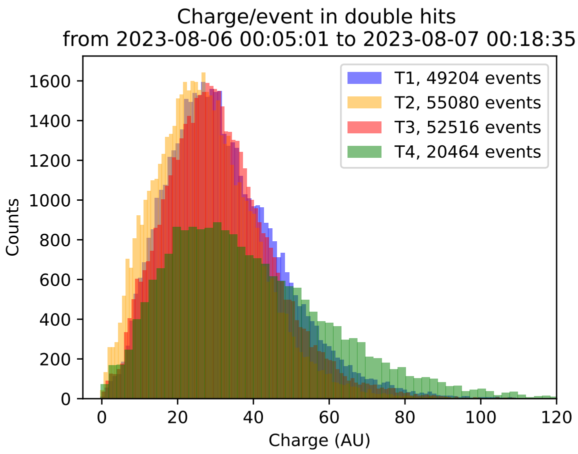

Figure 11. Charge spectrum per RPC for charge collected in double hits. Note how the bell shape of the spectrum is recovered compared to the stripwise study. Also, the spectrum of T4 is different in profile to those in other layers, suggesting a slight shift of the mean charge of the detections to higher energies.

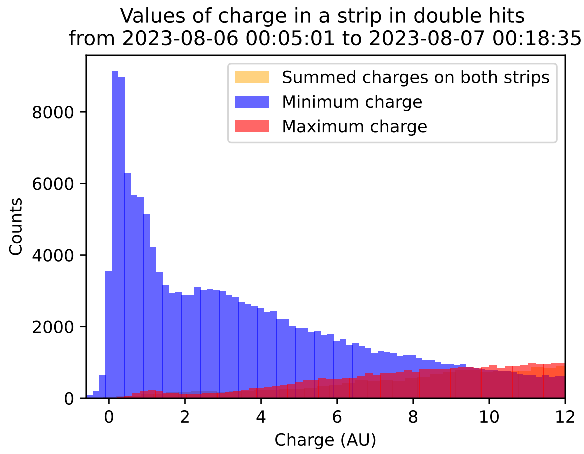

Figure 12. Values of charge collected per strip in double hits for the minimum, maximum and total charge. Note the bimodal distribution on the minimum charge spectrum: the left peak is due to crosstalk, the right curve is the distribution of charge actually shared between strip in what could be an actual interstrip detection.

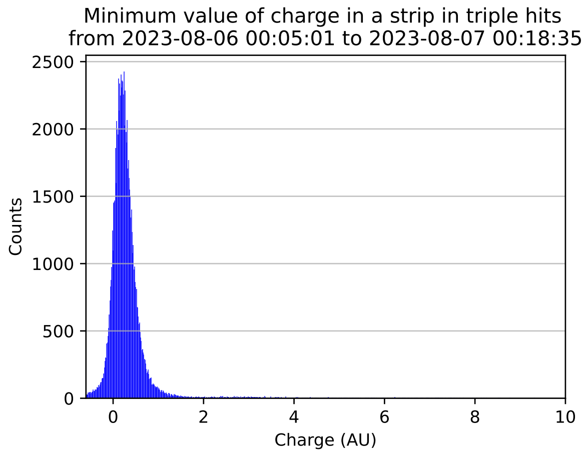

Figure 13. The minimum values of charge collected per strip in each detection in triple hits. From this study 1.75 AU of charge is taken as an upper bound for the interstrip.

If the representation is, instead of strip-wise, summing all the strips, then it can be seen in Fig. 11 how the shape of the spectra is recovered.

This indicates clearly that the crosstalk is not so predominant in double hits as the pure interstrip effect: it is essential to sum the charge collected in different strips to get the original charge of the events. It is also interesting to note that the larger number of single hits in T2 is now compensated by a very low number of double hits in T2 compared to the other RPCs.

Actually the crosstalk can be easily differentiated from the splitting of charge between strips taking a look closely to the small values of the distribution made with the minimum values of charge collected in each double hit:

Plotting the minimum values of the charge collected in each triple hit, in Fig. 13, or the minimum values of the charge collected in quadruple hits also helps discriminate the distribution of crosstalk charge.

Also checking in double hits the distribution of fractional charged shared between both strips can give interesting information. Fig. 14 displays this behaviour. Two different phenomena can be easily distinguished in this plot. On the one hand, the extreme values, around 0 and 1, are by far the most frequent: this is the case in which a great part of the charge is in one of both strips, so those events can be associated to **crosstalk**. On the other hand, every other fraction of charge that is not around those extremes shows a smooth behaviour in distribution, suggesting its association with an **interstrip** event.

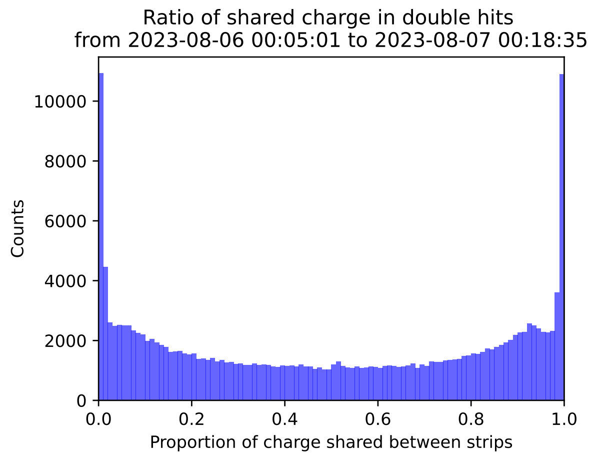

Figure 14. Ratio of shared charge in each double hit between two adjacent strips.

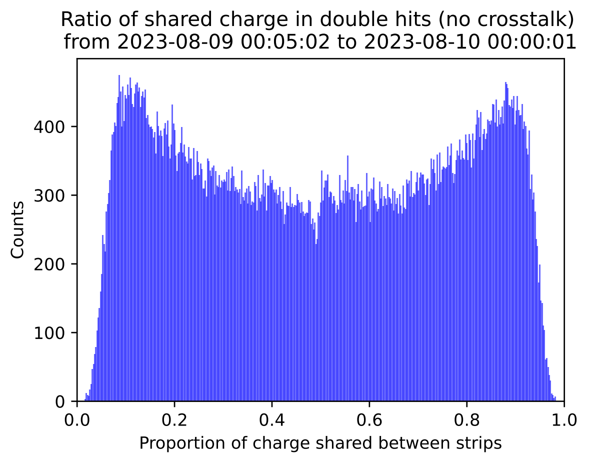

Figure 15. Ratio of shared charge in each double hit removing crosstalk.

This allows to design a selection criteria to determine when a multistrip detection can be considered a interstrip hit: check if the charge values different from zero are in consecutive strips, then check that the positions of the hit in those two strips are not too far (because that would suggest a multiplicity $n > 1$ event), see if any of the values is between what can be considered the crosstalk range (from 0 to 1.75, approximately) and check if the difference of the two charges is not too high (since it could imply a a higher multiplicity event).

Filtering the charges according to this criteria to remove the crosstalk charges the distribution of shared charge displayed in Fig. 15 can be obtained.

4.3.4 Multiplicity study

A simple method to set bounds on high multiplicity events, those in which several particles participate, has been implemented. Further work is needed, but the main scheme

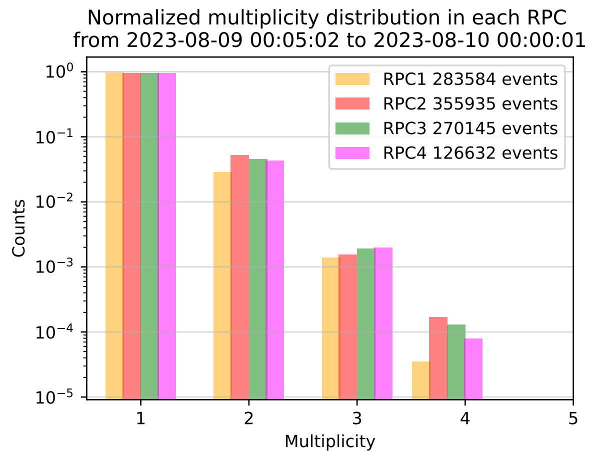

Figure 16. Multiplicity distribution according to the RPC. Note how small the number of multiplicity $n = 2$ events is compared to that of double strip hits in Fig. 9

is already defined. The algorithm takes the information of a detection in a RPC and checks if there is any strip triggered (else $n = 0$). If there is only one strip triggered, it is considered a $n = 1$ detection. If there are two, then the algorithm checks if both are close along the strip and also if they are in consecutive strips (else $n = 2$), then if one of the charges can be associated with crosstalk or with an interstrip detection it is considered $n = 1$. If there are three strips triggered it checks if they are consecutive, else the isolated is considered a count and the double strip algorithm just explained is applied to those two strips. If the three strips triggered are in fact consecutive then it needs to be seen if some of the charges can be associated with crosstalk, etc. Many cases can take place, but the core idea of the algorithm is maintained. This allows a first, naive calculation that leads to Fig. 16.

4.4 Future work

In the pursuit of enhancing the capabilities of our cosmic ray telescope, several avenues of work remain pending. One of our primary objectives is the development of a comprehensive database and query system. Such a system will streamline data retrieval and analysis processes, facilitating more efficient and focused research endeavors and making the data accessible to the groups working in the CASTRO collaboration.

Additionally, the optimization of interstrip measurement represents a crucial aspect awaiting thorough implementation. Accurate interstrip measurements hold the potential to significantly enhance our instrument's precision and resolution, contributing to a more refined understanding of cosmic ray interactions.

Furthermore, our efforts are directed towards performing a comprehensive multiplicity study that includes also not only the number of particles involved, but the topology of the event, trying to obtain, if possible, the decay point and the remnants, as well as estimating the energy of the incident secondary cosmic ray.

Last but not least, a robust, realistic, temperature independent cosmic ray rate calculation is set as a main objective for the near future, being this the first proper scientific result the telescope can give.

5 Conclusion

The miniTRASGO cosmic ray telescope introduces an innovative approach to the study of cosmic rays, harnessing advanced technologies for data acquisition and analysis. Its versatile design, incorporation of RPCs, and capability to measure both muons and electrons offer a new perspective on UHECRs and cosmic ray interactions. The ongoing efforts to establish a database, enhance interstrip measurements, investigate multiplicity, and calculate a more realistic cosmic ray rate underscore the telescope's potential to significantly contribute to our understanding of cosmic phenomena. Continued improvements to miniTRASGO's capabilities promise further insights into the complex realm of cosmic rays.

Acknowledgments

Many thanks to Alberto Blanco for his attention, both in the weeks we have spent in Coimbra and remotely, and for his careful and tireless work in teaching us how to do, *hands on*, the best job possible.

References

[1] M. Xarepe, T. Aumann, A. Blanco, A. Corsi, D. Galaviz, H.T. Johansson, S. Linev, B. Löher, L. Lopes, J. Michel, V. Panin, D. Rossi, J. Saraiva, H. Törnqvist, M. Traxler, *Resistive plate chambers for precise measurement of high-momentum protons in short range correlations at R3B*, *Nuclear Instruments and Methods in Physics Research Section A: Accelerators, Spectrometers, Detectors and Associated Equipment*, vol. 1055, pp. 168445, 2023, ISSN: 0168-9002, DOI: https://doi.org/10.1016/j.nima.2023.168445, URL: https://www.sciencedirect.com/science/article/pii/S0168900223004357

[2] E Cerron Zeballos, I Crotty, D Hatzifotiadou, J Lamas Valverde, S Neupane, M.C.S Williams, A Zichichi, *A new type of resistive plate chamber: The multigap RPC*, *Nuclear Instruments and Methods in Physics Research Section A: Accelerators, Spectrometers, Detectors and Associated Equipment*, vol. 374, no. 1, pp. 132-135, 1996, ISSN: 0168-9002, DOI: https://doi.org/10.1016/0168-9002(96)00158-1, URL: https://www.sciencedirect.com/science/article/pii/0168900296001581

[3] D. Belver, P. Cabanelas, E. Castro, J. A. Garzón, A. Gil, D. Gonzalez-Diaz, W. Koenig, M. Traxler, *Performance of the Low-Jitter High-Gain Bandwidth Front-End Electronics of the HADES tRPC Wall*, *IEEE Transactions on Nuclear Science*, vol. 57, no. 5, pp. 2848-2856, 2010, DOI: 10.1109/TNS.2010.2056928

[4] Andreas Neiser, J. Adamczewski-Musch, Matthias Hoek, Wolfgang Koenig, Grzegorz Korcyl, Sergey Linev, Ludwig Maier, Jan Michel, Marek Palka, *TRB3: a 264 channel high precision TDC platform and its applications*, *Journal of Instrumentation*, vol. 8, no. 12, pp. C12043, 2013, Publisher: IOP Publishing

[5] J. Linsley, *Mini and super mini arrays for the study of highest energy cosmic rays*, *19th Intern. Cosmic Ray Conf. La Jolla*, vol. 3, pp. 434-437, August 1985.

[6] D. Belver, et al., *Analysis of the space-time microstructure of cosmic ray air showers using the HADES RPC TOF wall*, *JINST*, vol. 7, pp. P10007, 2012.

[7] D. Belver, P. Cabanelas, D. Domínguez, Juan A. Garzón, G. Kornakov, M.F. Morales, *TRASGO: A proposal for a timing RPCs based detector for analyzing cosmic ray air showers*, *Nuclear Instruments and Methods in Physics Research Section A: Accelerators, Spectrometers, Detectors and Associated Equipment*, vol. 661, pp. S163-S167, 2012, Note: X. Workshop on Resistive Plate Chambers and Related Detectors (RPC 2010), ISSN: 0168-9002, DOI: https://doi.org/10.1016/j.nima.2010.09.173, URL: https://www.sciencedirect.com/science/article/pii/S0168900210022084, Keywords: Timing RPCs, Cosmic rays, Extended air showers, Tracking detectors,

[8] D. García-Castro, M. Ajoor, H. Alvarez-Pol, et al., *The TRASGO Project. Present Status and Results*, *Phys. Atom. Nuclei*, vol. 84, pp. 1070–1079, 2021, DOI: https://doi.org/10.1134/S1063778821130093.